PART FIVE

HOIST SHAFT MINE COMMUNICATIONS

PART FIVE

HOIST SHAFT MINE COMMUNICATIONS

TABLE OF CONTENTS

PART FIVE

HOIST SHAFT MINE COMMUNICATIONS

LIST OF TABLES

PART FIVE

HOIST SHAFT MINE COMMUNICATIONS

LIST OF FIGURES

PART FIVE

HOIST SHAFT MINE COMMUNICATIONS

INTRODUCTION

During the summer of 1973 we were asked to perform a theoretical investigation of the propagation of low frequency (LF) radio waves down deep (10,000 feet) hoist shafts* for the case where the hoist cable ("rope") is the only metal conductor present. Propagation is by means of the TEM coaxial mode of transmission in which the hoist cable serves as the inner conductor and the surrounding rock acts as the outer conductor.

Since the rock is a relatively poor electrical conductor the current in the outer conductor of the coaxial line is not confined to a very thin surface layer as in a metal coaxial cable, but spreads radially to a distance that is generally many times the shaft diameter. This feature of the wave propagation requires a more sophisticated theoretical treatment than the approximate skin-depth theory that is adequate for metal coaxial lines.

In this Part we treat the hoist shaft wave propagation loss, characteristic impedance, and the field current distributions in the surrounding rock medium. We also show that the large penetration of the wave into the rock outer conductor does not present a difficult problem with regard to coupling the transmitter or receiver to the transmission line with a minimum of insertion loss, but that the large impedance mismatch caused by the capacitance termination between the cage and shaft wall may well be the most significant contribution to overall system loss. Inductive coupling and impedance matching to the hoist rope/shaft transmission line are also treated briefly. Preliminary results indicate that a broad minimum in overall system loss should occur between 100 kHz and 1 MHz, possibly centered around 300 kHz. Further work is needed to better quantify this signal loss behavior, compare it with hoist shaft electromagnetic noise spectral data recently acquired by NBS, and identify the most favorable operating frequencies.

---

*This work complemented the hardware development of a new hoist radio system for deep shafts by Collins Radio Co. under Contract H0232056 for the Bureau of Mines.

I. THE MODE CONDITION

We approximate the actual rectangular shaft by a cylinder of circular cross-section of radius b containing a steel cable of radius a along its axis. The dominant mode of propagation in such a transmission line has a radially-symmetric transverse magnetic field H_θ which, for $a \leq r \leq b$ has the form

$$H_\theta = [AJ_1(k_r r) + B\, Y_1(k_r r)]\, e^{-ik_z z} \qquad (1)*$$

where A and B are arbitrary constants and J_1 and Y_1 are first order Bessel functions of the first and second kind, respectively. The radial and longitudinal wave vector components k_r and k_z satisfy the condition

$$k_r^2 + k_z^2 = k_o^2 = \frac{4\pi^2}{\lambda^2} \qquad (2)$$

where λ is the free space wavelength.

The electric field components are given by the curl components

$$E_r = -\frac{1}{i\omega\varepsilon_o}\frac{\partial H_\theta}{\partial z} \qquad (3)$$

$$E_z = \frac{1}{i\omega\varepsilon_o}\frac{1}{r}\frac{\partial}{\partial r}(rH_\theta) \qquad (4)$$

which, from (1) and the properties of the Bessel functions, give

$$E_r = \frac{ik_z}{i\omega\varepsilon_o}[AJ_1(k_r r) + BY_1(k_r r)]e^{-ik_z z} \qquad (5)$$

$$E_z = \frac{k_r}{i\omega\varepsilon_o}[AJ_o(k_r r) + BY_o(k_r r)]e^{-ik_z z} \qquad (6)$$

The fields given by (1), (5), and (6) represent an exact solution of Maxwell's equations.

---

* References to Figures, Tables, and Equations apply to those in this Part unless otherwise noted.

In the conducting rock surrounding the shaft ($r > b$) the radial part of the solution must correspond to an outgoing traveling wave. The solution therefore has the form

$$H_\theta = C\, H_1^{(2)}(k_r' r) e^{-ik_z z} \tag{7}$$

$$E_r = \frac{ik_z}{i\omega\varepsilon} C\, H_o^{(2)}(k_r' r) e^{-ik_z z} \tag{8}$$

$$E_z - \frac{k_r'}{i\omega\varepsilon} C\, H_o^{(2)}(k_r' r) e^{-ik_z z} \tag{9}$$

where $H_1^{(2)}$ and $H_o^{(2)}$ are the Hankel functions given by

$$H_1^{(2)} = J_1 - iY_1 \tag{10}$$

$$H_o^{(2)} = J_o - iY_o \tag{11}$$

C is an arbitrary constant, ε is the complex permittivity of the rock, and k_r' is given by the relation

$$k_r'^2 + k_z^2 = K k_o^2 \tag{12}$$

where $K = \varepsilon/\varepsilon_o$ is the complex dielectric constant of the rock.

At the wall of the shaft the boundary conditions that H_θ and E_z are continuous give the relations

$$A\, J_1(k_r b) + B\, Y_1(k_r b) = C\, H_1^{(2)}(k_r' b) \tag{13}$$

$$k_r [A\, J_o(k_r b) + B\, Y_o(k_r b)] = \frac{k_r'}{K} C\, H_o^{(2)}(k_r' b) \tag{14}$$

At the inner conductor (r = a) the conductivity of the steel is so high that the boundary condition is simply $E_z = 0$. Therefore from (6),

$$A\, J_o(k_r a) + B\, Y_o(k_r a) = 0. \tag{15}$$

Equations (13), (14), and (15) are homogeneous in A, B and C. The requirement for consistency of these equations gives the mode condition

$$\frac{1}{k_r}\left[\frac{\frac{J_1(k_r b)}{J_o(k_r a)} - \frac{Y_1(k_r b)}{Y_o(k_r a)}}{\frac{J_o(k_r b)}{J_o(k_r a)} - \frac{Y_o(k_r b)}{Y_o(k_r a)}}\right] = \frac{K}{k_r'}\,\frac{H_1^{(2)}(k_r' b)}{H_o^{(2)}(k_r' b)} \tag{16}$$

Equations (16), (2) and (12) determine exactly the allowed values of k_r, k_z and k'_r for all modes of propagation having a transverse axially-symmetric magnetic field. We are only interested in the lowest such mode, which approximates a TEM mode.

II. PROPAGATION LOSS

For frequencies in the range 20-200 kHz, $k_r a$, $k_r b$ and $k'_r b$ are all small quantities. Therefore the Bessel functions in (16) can be approximated by the first terms in their series expansions, namely

$$J_o(x) = 1 \tag{17}$$

$$J_1(x) = \frac{x}{2} \tag{18}$$

$$Y_o(x) = \frac{2}{\pi}(\log x + 0.577 - \log 2) \tag{19}$$

$$Y_1(x) = -\frac{2}{\pi x} \tag{20}$$

$$H_o^{(2)}(x) = 1 - \frac{2i}{\pi}(\log x + 0.577 - \log 2) \tag{21}$$

$$H_1^{(2)}(x) = \frac{2i}{\pi x} \tag{22}$$

Equation (16) then reduces to

$$k_r^2 = \frac{\pi i k_r'^2}{2K \log \frac{b}{a}} \left[1 - \frac{2i}{\pi} (\log k_r' b + 0.577 - \log 2)\right] \qquad (23)$$

The dielectric constant of a conducting medium is given approximately by the relation

$$K = - \frac{i\sigma}{\omega \varepsilon_o} \qquad (24)$$

For the case σ = 0.01 mho/m and f = 50 kHz, K = -3597 i. Therefore from (12), to a very good approximation,

$$k_r'^2 = K k_o^2 \qquad (25)$$

since k_r^2 is of the same order as k_o^2 and can therefore be neglected compared with $K k_o^2$. On substituting this value of $k_r'^2$ into (23), and then solving (2) for k_z^2, we find that

$$k_z^2 = k_o^2 \left[1 - \frac{\pi i}{2 \log \frac{b}{a}} - \frac{1}{\log \frac{b}{a}} (\log k_o b\sqrt{K} + 0.577 - \log 2)\right. \qquad (26)$$

We take the following values of the constants:

$$\begin{aligned} f &= 50 \text{ kHz} \\ \lambda &= 6{,}000 \text{ m} \\ k_o &= 1.047 \times 10^{-3} \text{ m}^{-1} \\ b &= 4 \text{ ft.} = 1.2 \text{ m} \\ a &= 0.875 \text{ in.} = 0.0222 \text{ m} \\ \sigma &= 0.01 \text{ mho/m} \\ \varepsilon_o &= 8.85 \times 10^{-12} \text{ farad/m} \\ K &= -3597 \text{ i} \end{aligned}$$

Then we find

$$k_z = 1.358 \times 10^{-3} - 7.948 \times 10^{-5} i \ (m^{-1})$$

For a 10,000 foot shaft (3050m), the propagation loss is therefore

$$L = (8.686)\ (7.948 \times 10^{-5}\ m^{-1})\ (3050m) = 2.11\ dB$$

III. SURFACE IMPEDANCE METHOD

An alternative way to calculate the propagation loss is by means of the surface impedance Z_s of the wall of the shaft which is defined as

$$Z_s = - \frac{E_z(b)}{2\pi b\ H_\theta(b)} \tag{27}$$

From (7) and (9) this becomes

$$Z_s = \frac{ik_r'}{2\pi b\omega\varepsilon} \frac{H_o^{(2)}(k_r'b)}{H_1^{(2)}(k_r'b)} \tag{28}$$

With the same approximations as before this becomes

$$Z_s = \frac{k_o^2}{4\omega\varepsilon_o} \left[1 - \frac{2i}{\pi} (\log k_o b\sqrt{K} + 0.577 - \log 2)\right] \tag{29}$$

We now insert Z_s as a series impedance into the usual transmission line formula for the propagation constant:

$$\gamma = \sqrt{(R + i\omega L)\ (G + i\omega C)} \tag{30}$$

to obtain the formula

$$\gamma = \sqrt{(Z_s + i\omega L)\ i\omega C} \tag{31}$$

where we assume that the resistance R per unit length of the inner conductor is negligible compared with Z_s and that there is no shunt conductance.

Since

$$\gamma^2 = -k_z^2 , \tag{32}$$

$$L = \frac{\mu_o}{2\pi} \log \frac{b}{a} , \tag{33}$$

$$C = \frac{2\pi\varepsilon_o}{\log \frac{b}{a}} \tag{34}$$

$$k_o^2 = \omega^2 \varepsilon_o \mu_o , \tag{35}$$

where $u_o = 4\pi x 10^{-7}$ henry/m.

Equation (31) becomes

$$k_z^2 = k_o^2 - \frac{2\pi i\omega\varepsilon_o Z_s}{\log \frac{b}{a}} \tag{36}$$

This formula becomes identical with Equation (26) when the expression (29) is substituted for Z_s.

Table 1 gives values of Z_s calculated by means of Equation (29) for frequencies in the range 30-3,000 kHz and conductivities in the range 10^{-4} to 10^{-1} mho/m. It is of interest that the real part of the surface impedance $R_s = \omega\mu_o/8$, is independent of the conductivity and the radius of the shaft. The value of Z_s for 3,000 kHz and 0.01 mho/m is somewhat uncertain, since the approximations used are near the limit of their validity for these values.

Table 1

Surface Impedance

Z_s (ohm/m) for b = 1.2 m = 4 ft.

f (kHz) \ σ (mho/m)	10^{-4}	10^{-3}	10^{-2}	10^{-1}
30	.0296 + .1982i	.0296 + .1548i	.0296 + .1114i	.0296 + .0680i
50	.0493 + .3141i	.0493 + .2418i	.0493 + .1695i	.0493 + .0973i
100	.0986 + .5847i	.0986 + .4402i	.0986 + .2956i	.0986 + .1511i
150	.1479 + .8389i	.1479 + .6221i	.1479 + .4053i	.1479 + .1885i
200	.1972 + 1.0824i	.1972 + .7933i	.1972 + .5043i	.1972 + .2152i
250	.2465 + 1.3180i	.2465 + .9567i	.2465 + .5953i	.2465 + .2340i
300	.2958 + 1.547i	.2958 + 1.114i	.2958 + .6801i	.2958 + .2464i
3000	2.958 + 11.14i	2.958 + 6.801	2.958 + 2.465i	----------

The resistance of the stainless steel center conductor of radius 0.0222m and conductivity 10^6 mho/m is given in Table 2. The results include the effect of the skin depth of penetration into the cable. It is seen that the cable resistance is small compared with the real part of the surface impedance given in Table 1 at all frequencies, and therefore has little effect on propagation loss.

Table 2

Resistance of Center Conductor for
$a = .0222m$, $\sigma = 10^6$ mho/m

f (kHz)	R (ohm/m)
30	.0025
50	.0032
100	.0045
150	.0055
200	.0064
250	.0071
300	.0078
3000	.0246

Table 3 gives the propagation loss in dB for the same range of frequency and conductivity, calculated by means of Equation (36) for a 10,000 foot shaft. It is seen that the loss is very low at 30 kHz and quite moderate at 300 kHz. However the loss is excessive at 3,000 kHz. It is to be noted that the loss is almost independent of conductivity.

Table 3

Propagation Loss, L(dB)

(for b = 1.2m, a = 0.0222m, z = 3050m)

f (kHz) \ σ (mho/m)	10^{-4}	10^{-3}	10^{-2}	10^{-1}
30	1.1	1.1	1.2	1.4
50	1.8	1.9	2.1	2.3
100	3.7	4.0	4.3	4.8
150	5.6	6.1	6.6	7.3
200	7.6	8.1	8.9	9.9
250	9.5	10.3	11.2	12.5
300	11.5	12.4	13.6	15.0
3000	124.1	135.7	151.4	--

IV. CHARACTERISTIC IMPEDANCE

The characteristic impedance of a transmission line is given by the expression

$$Z_o = \sqrt{\frac{R + i\omega L}{G + i\omega C}} \tag{37}$$

In the case of the shaft transmission line G = 0 and R = Z_s, which is the surface impedance given by Equation (29) or Table 1. Then (37) becomes,

$$Z_o = \sqrt{\frac{Z_s + i\omega L}{i\omega C}} \tag{38}$$

where L and C are given by (33) and (34).

For f = 100 kHz and $\sigma = 10^{-3}$ mho/m, we find that Z_s = 0.0986 + 0.4402i ohm/m, $i\omega L$ = (0.501) i ohm/m, $i\omega C = (8.76 \times 10^{-6})$ $i(\text{ohm/m})^{-1}$, and Z_o = 327 - 17 i ohms. For $\sigma = 10^{-2}$ mho/m, we get:

Table 4

Characteristic Impedance
(for $\sigma=10^{-2}$ mho/m, b=1.2 m, a=0.0222 m)

f (kHz)	Z_o (ohms)
50	310-18i
300	283-20i

For comparison, Z_o = 239 ohms for an all-metal transmission line with the same dimensions.

V. CURRENT DISTRIBUTION IN THE SURROUNDING MEDIUM

From Equation (7) the magnetic field in the rock is given by

$$\frac{H_\theta(r)}{H_\theta(b)} = \frac{H_1^{(2)}(k_r'r)}{H_1^{(2)}(k_r'b)} \tag{39}$$

The current density is therefore given by

$$\frac{J_z(r)}{J_z(b)} = \frac{\frac{1}{r}\frac{\partial}{\partial r}(rH_\theta)}{J_z(b)} = \frac{H_o^{(2)}(k_r'r)}{H_o^{(2)}(k_r'b)} \tag{40}$$

Although $k'_r r$ is small compared with 1 at the wall of the shaft, this is not true for larger values of r where the current density is still appreciable. Therefore we cannot now use only the first term of the expansion of the Hankel function. However, since, from (24) and (25), k_r' has equal real and imaginary parts, we can write

$$k_r'r = xe^{-\pi i/4} \tag{41}$$

and use the tabulated functions* ker (x) and kei(x) to obtain the real and imaginary parts of the Hankel function. The relationships are

$$\text{ker}(x) = \text{Re}\left[-\frac{\pi i}{2} H_o^{(2)}(xe^{-\pi i/4})\right] \tag{42}$$

$$\text{kei}(x) = \text{Im}\left[-\frac{\pi i}{2} H_o^{(2)}(xe^{-\pi i/4})\right] \tag{43}$$

where

$$x = |k_r'|r \tag{44}$$

---

* Handbook of Mathematical Functions, Ed. M. Abramowitz and I.A. Stegun, National Bureau of Standards, U.S. Department of Commerce, June 1964, p. 431.

from (41) above, so that

$$J_z(x) = J_{real}(x) + iJ_{imag}(x) \tag{45}$$

where $J_{real}(x) \propto \text{ker}(x)$ and $J_{imag}(x) \propto \text{kei}(x)$

Of particular interest to the coupling of signals to the shaft is the cumulative distribution of vertical current in the rock as a function of radial distance, r.

$$I_z(r) = \int_b^r 2\pi r\, J_z(r)\, dr \tag{46}$$

Therefore we have computed the dimensionless quantity

$$I(x) = \sqrt{I^2_{real} + I^2_{imag}} \tag{47}$$

which is proportional to $I_z(r)$, where

$$I_{real} = \int_{x_o}^{x} \frac{x\, J_{real}(x)\, dx}{x_o\, J_{real}(x_o)} \tag{48}$$

$$I_{imag} = \int_{x_o}^{x} \frac{x\, J_{imag}(x)\, dx}{x_o\, J_{real}(x_o)} \tag{49}$$

and $$x_o = |k_r'|b \tag{50}$$

The quantities $\frac{x\, J_{real}(x)}{x_o\, J_{real}(x_o)}$ and $\frac{x\, J_{imag}(x)}{x_o\, J_{real}(x_o)}$, which are proportional to the real and imaginary parts of the current flowing in an annulus of infinitesimal width dx at radius x, are plotted in Figure 1, while the quantity I(x) is plotted in Figure 2.

In each plot, the dimensionless radius of the shaft wall, x_o, has been set equal to 0.1. In view of equation (50), for a shaft radius b = 4 feet = 1.2 meters, x = 0.1 corresponds to a $k_r = 0.083\ m^{-1}$. Since $|k_r'| = k_o \sqrt{|K|}$ and $k = -\frac{i\sigma}{\omega\varepsilon_o}$ this means that for a rock conductivity σ = 0.01 mho/m, the corresponding frequency is equal to 87 kHz and K = -2067i. Other combinations of f, σ, and b will produce different values of x_o.

VI. COUPLING TO THE TRANSMISSION LINE

The overall communication efficiency between transmitter/receiver units located on the surface and in the cage will be influenced not only by the line attenuation loss. It will also depend on the losses caused by the methods used to establish the return current path in the rock, and more importantly on the losses due to impedance mismatches and standing waves. These latter losses will be caused by the high impedance capacitive termination at the cage end of the line, the low resistance sheave wheel grounding termination on the surface, and the couplers used to inductively couple signals onto the transmission line via the hoist rope.

A. Spatial Coupling Factors for the Return Paths.

Examination of Figure 2 reveals that the return current is widely distributed in the rock for typical values of b = 1.2m, σ = 0.01 mho/m, and f = 87 kHz. At first this would seem to imply that low loss coupling from the transmitter into the fundamental transmission-line mode requires a system of return-current electrodes implanted in the ground over a circular area of diameter equal to about 10-20 hoist-shaft diameters. We will now show, however, that the loss is actually quite small even when the area covered by the electrodes is only comparable with the cross-sectional area of the shaft itself.

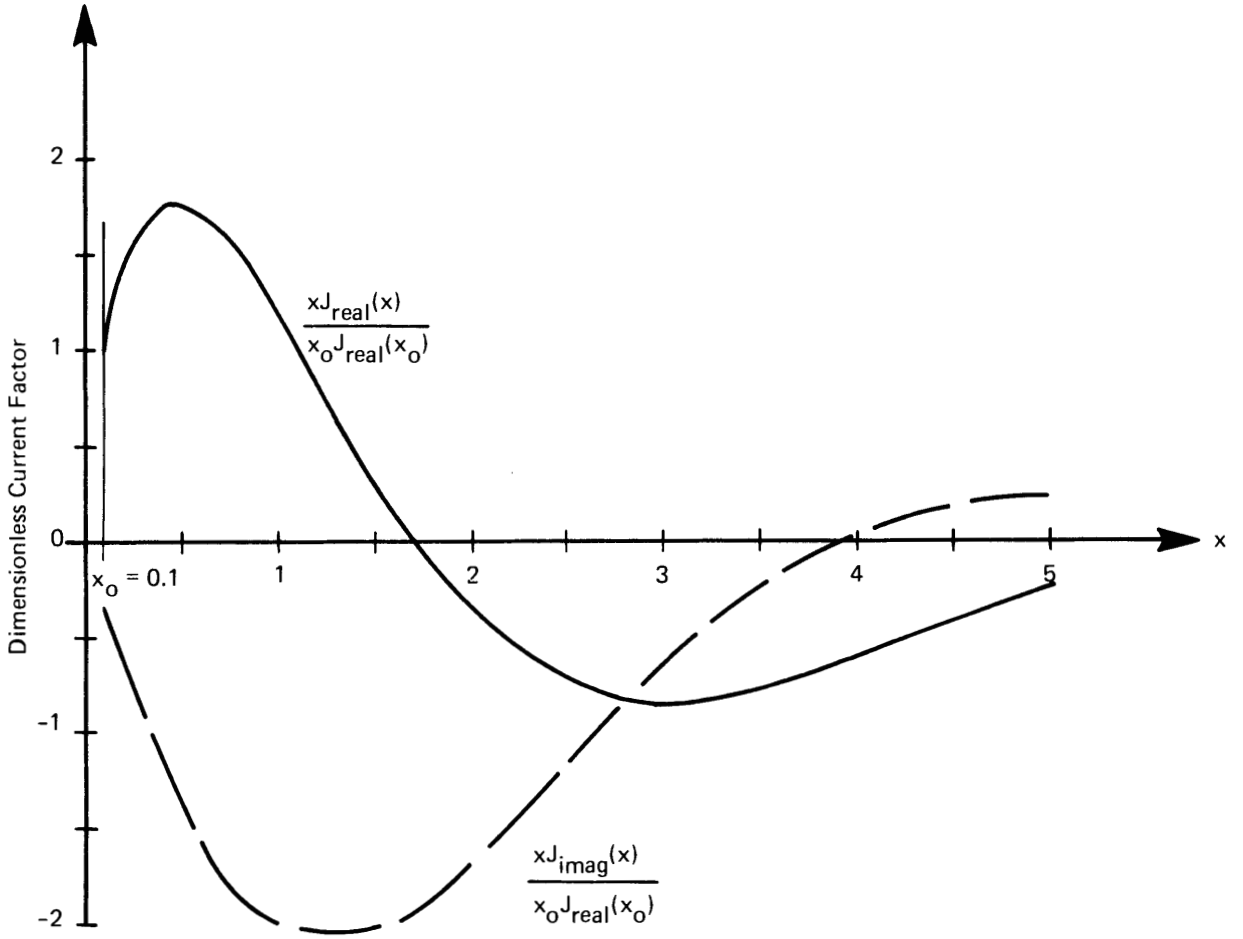

FIGURE 1 DIMENSIONLESS CURRENT FACTORS FOR ANNULUS AT RADIUS X

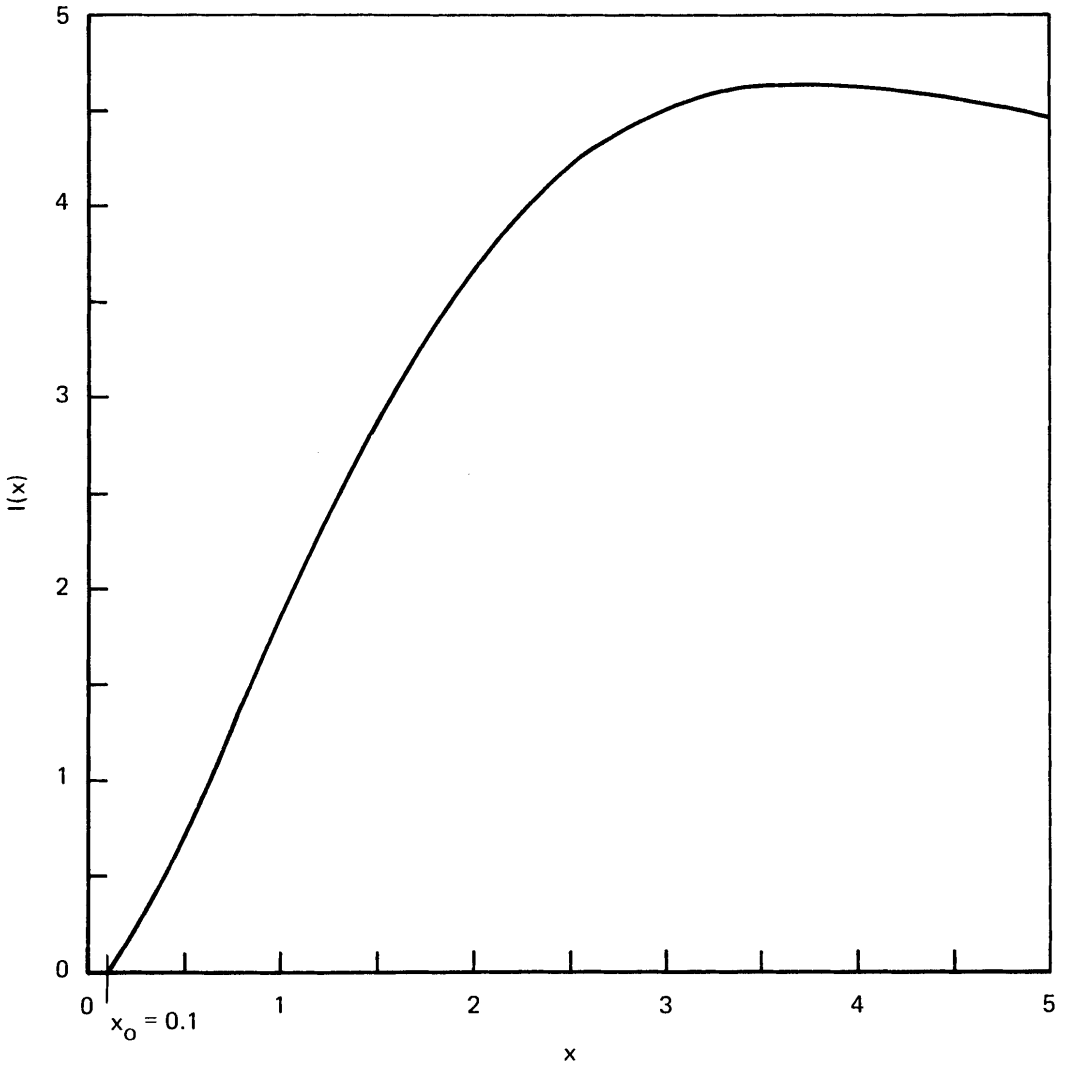

FIGURE 2 DIMENSIONLESS CUMULATIVE CURRENT I(x) VERSUS x

The argument is that we can divide this coupling problem into two parts, the first being concerned with current flow from an electrode out to about one skin-depth, and the second having to do with the transition from this region, of essentially spherical spreading (or converging) of the current, to the region of transmission-line propagation beyond one skin-depth, in which the current flow is mainly in the z-direction.

In the first region the current flow pattern is approximately like that of direct current from a hemispherical electrode embedded in a semi-infinite resistive medium, with its flat face flush with the surface of the medium. The current flow in this case is radial, and the total resisttance to flow is contributed almost entirely by the volume within a few hemisphere radii. The spreading resistance is

$$R_s = \frac{1}{2\pi a_o \sigma} , \qquad (51)$$

where a_o is the radius of the hemisphere and σ is the conductivity of the rock.

The spreading resistance is not very sensitive to the exact electrode shape. A shape of interest in the hoist problem, at both the transmitter and receiver, is that of a hollow cylindrical electrode of length ℓ in contact with the wall of the shaft. In practice, such an electrode at the surface end of the shaft will most likely be approximated by three or more roof bolts connected in parallel and driven into the wall of the shaft, equally spaced around its perimeter. At the cage end, the "electrode" will be a cylindrical capacitance "connection" formed by the air space between the outer walls of the cage and the walls of the shaft. At the transmitter, the cylinder will act approximately like the above mentioned hemisphere having the same area of curved surface as the cylinder. The equivalent hemispherical radius is then

$$a_o = \sqrt{b\ell} , \qquad (52)$$

where b is the shaft radius. For σ = 0.01 mho/m, b = 1.2 m, ℓ = 3 m, we find from (51) and (52) that R_s is only 8.4 ohms. This resistance is in series with the characteristic impedance of the transmission line, which has a real part of about 300 ohms. Therefore, for σ = .01 ohm/m, the spreading resistance has negligible effect. For σ = .001 ohm/m, R_s is 84 ohms, and should be allowed for in the design of the driving circuit.

At the receiver the equivalent shpere radius is $a_o = \sqrt{b\ell/2}$ but the spreading resistance is now $1/(4\pi a_o \sigma)$. Thus, the spreading resistance is lowered by a factor of 2. This resistance is in series with the capacitive reactance between the cage and the shaft wall as well as with the characteristic impedance of the transmission line.

We now turn to the transition from spherical spreading to the transmission line mode of current flow. For simplicity we assume that the transition occurs sharply at the plane z = δ, where δ is the skin-depth given by the formula

$$\delta = \sqrt{\frac{1}{\pi f \mu_o \sigma}} . \tag{53}$$

For the values f = 87 kHz and σ = 0.01 mho/m corresponding to b = 1.2 m and x_o = 0.1, as in Figures 1 and 2, we find that δ = 17 m.

In the spherical-spreading region the current density depends on the spherical radius r_s according to the relation

$$j = \frac{A}{r_s^2} , \tag{54}$$

where A is an arbitrary constant. On the plane z = δ the z = component of j is given by

$$j_z(r) = \frac{A\delta}{(\delta^2 + r^2)^{3/2}}, \tag{55}$$

where r is the cylindrical radial coordinate.

We regard $j_z(r)$ as driving the various modes of the transmission line. The power coupling constant C for the fundamental TEM mode is given by the formula

$$C = \frac{\left| \int_b^\infty J_z^* \, j_z \, rdr \right|^2}{\int_b^\infty |J_z|^2 rdr \int_b^\infty |j_z|^2 rdr} , \qquad (56)$$

where J_z is the z - component of current density in the transmission line mode. The numerator is the overlap integral between J_z and j_z. The integrals in the denominator are normalizing factors. It is seen that when j_z has the same r-dependence as J_z, C=1. On the other hand, when j_z is orthogonal to J_z, C=0.

On changing to the dimensionless variable x given by (44) and substituting from (40) for $J_z(r)$ and from (55) for j_z we find approximately on expressing the result in terms of the ker and kei functions (Equations 42 and 43);

$$C = \frac{4 \left(\frac{x_o \delta}{b}\right)^4 \left\{ \left(\int_{x_o}^\infty \frac{\ker(x)\, xdx}{\left[\left(\frac{x_o \delta}{b}\right)^2 + x^2\right]^{3/2}} \right)^2 + \left(\int_{x_o}^\infty \frac{\mathrm{kei}(x)\, xdx}{\left[\left(\frac{x_o \delta}{b}\right)^2 + x^2\right]^{3/2}} \right)^2 \right\}}{\int_{x_o}^\infty \left[(\ker(x))^2 + (\mathrm{kei}(x))^2\right] xdx} . \qquad (57)$$

On taking $x_o = 0.1$, $\delta = 17$ m, and b = 1.2 m, we find by numerical integration of the integrals in (57) that C = 0.7 = -1.5 dB.

Therefore, the initial spherical spreading of the current, over a distance of the order of a skin depth (from relatively small electrodes such as the above mentioned cylindrical electrode approximations for the surface ground connection and the cage capacitive coupling geometries) yields a current distribution that matches the fundamental mode shape quite well, thereby contributing only a very small loss factor. Taken together with the relatively small spreading resistance effects, the losses due to spatial coupling factors for the return current path will not be major contributors to overall system loss at the frequencies of interest.

B. Cage Capacitive Termination

First order calculations for the cage-to-shaft-wall capacitance yield values between 110 and 460 pf. The smaller of these values is the free space capacitance of a one-meter radius conducting sphere, while the larger is the capcitance between a 5.5 x 5.5 x 13 foot conducting box placed in an 8.8 x 8.8 foot conducting enclosure, neglecting fringing effects. Choosing a nominal capacitance value equal to the geometric mean, 224 pf, we obtain the following capacitive reactance values over the frequency range of interest (see Table 5).

Table 5

Capacitive Reactance of Cage Termination
(for C = 224 pf)

f (kHz)	X_C (Ohms)
10	71,000
30	24,000
50	14,000
100	7,100
300	2,400
500	1,400

At frequencies below about 100 kHz, this reactance in series with the nominal 300 ohm characteristic impedance of the lines will produce a large mismatch and standing wave voltage and current variations down the shaft. It will also produce substantial reductions in the signal voltages appearing across the transmitter/receiver units, which are in series with, and of considerably lower impedance than, the capacitive reactance of the cage at these frequencies. Two potential solutions to these problems are to raise the impedance levels of the transmitter/receiver units and to raise the operating frequency. The latter solution also helps to achieve the former, as will be discussed briefly in the next section.

C. Inductive Coupling and Impedance Matching to the Hoist Rope.

Since it is not feasible to place a break in the hoist rope to insert the surface and cage transmitter/receiver units, the signals must be inductively coupled onto and off the hoist rope/shaft transmission line. One way to accomplish this is through the use of ferrite or powdered iron toroidal core coupler/isolators similar to the one described in Chapter II of Part Six of this Volume, and shown in Figures 1 and 6 of that Chapter. In Part Six, the toroidal coupler/isolator with its associated capacitor is placed around the trolley pole drop wire, as shown in Figure 1A of Chapter II, to add impedance in series with the trolley motors at the trolley wire carrier phone frequency of 88 or 100 kHz. This is to prevent the trolley motors from acting as a signal "shorts" across the trolley wire transmission line. It also provides an alternative method for coupling the carrier phone to the trolley wire transmission line. The capacitor and optional resistor shown in these figures are used to tune the toroidal core isolator and adjust its Q, to obtain the desired impedance level and isolator selectivity at the frequency of interest.

This type of toroidal coupler/isolator should be applicable to hoist rope communication systems, first as a signal coupler and second as an impedance matching isolator. For example, at the surface end of the hoist rope it could be used not only to couple the transmitter/receiver units to the hoist rope-shaft transmission line, but to also add the appropriate amount of matching impedance in series with the low impedance sheave wheel/ground connectors, thereby preventing standing wave interference effects during cage to surface transmissions. At the cage end of the hoist rope, the role of the toroidal device will most likely be limited only to transmitter/receiver hoist rope coupling, because of the already large reactance termination presented by the cage-to-shaft wall capacitance, as given in Table 5.

The impedance levels obtainable from reasonably small coupler/isolator structures can be easily estimated by utilizing the design data established for the trolley motor isolator described in Chapter II of Part Six. For the same six pairs of I and U ferrite cores used in the isolator pictured in Figures 6 and 7 of that Chapter, Figure 7 reveals that for a nominal minimum air gap* of 0.005", the single-turn inductance will be 19 microhenries. The corresponding reactance and resonant impedance levels are given below in Table 6 of this section for the indicated selectivities. The 3 kHz bandwidth selectivity chosen for frequencies below 80 kHz is applicable to single sideband modulation, while the 12 kHz bandwidth chosen for frequencies above 80 kHz is applicable to narrowband frequency modulation.

Table 6

Inductive Reactance, Resonant Impedance, and Q
for a Small Single-Turn Toroidal Coupler/Isolator

		For 3 kHz Bandwidth		For 12 kHz Bandwidth	
(kHz)	(ohms)	Z_{res} (ohms)	Q	Z_{res} (ohms)	Q
10	1.2	4	3.3	-	-
20	2.4	16	6.7	-	-
40	4.8	64	13.3	16	3.3
80	9.6	256	26.7	64	6.7
160	19.2	-	-	256	13.3
320	38.4	-	-	1024	26.7

* A much larger air gap was required for the trolley wire carrier phone application, to prevent core saturation by the large DC currents flowing in the trolley wire to power the trolley motors.

Table 6 indicates that values of impedance comparable to the hoist rope transmission line characteristic impedance of about 300 ohms are easily achieved above 100 kHz, even for this small-sized isolator.* Consequently, larger toroidal coupler/isolators of this type should be investigated further for their potential application as couplers and impedance matching devices in hoist shaft communication systems.

VII. CONCLUDING REMARKS

As stated in Chapter VI of this Part, raising the operating frequency to above 100 kHz offers several advantages for reducing the overall system loss. For example, examination of Tables 3, 5, and 6 for propagation loss, cage reactance, and coupler impedance, respectively, reveals that operation at a frequency in the vicinity of 300 kHz should lead to substantially reduced overall loss over that obtainable at frequencies below 100 kHz or at frequencies above 1000 kHz. As the frequency is increased to around 300 kHz, the gain in signal voltage across the transmitter/receiver coupling units due to reduced cage reactance and increased coupler impedance, more than offsets the effects of increased propagation loss. However, these minima should be less severe (i.e., have a smaller VSWR) at the higher frequency of 300 kHz because of the greater difference in relative strengths of the incident and reflected waves (as a result of the higher attenuation rate along the transmission line and the smaller mismatches achievable for the cage and coupler impedances relative to the transmission line characteristic impedance).

---

* The outside dimensions of this particular isolator are 4-1/2" x 4-1/4" x 6", the inside dimension 1-1/4" x 2" x 6", making it too small, especially in cross-section, for use with the 1-3/4" diameter hoist rope application of interest. The hoist rope application requires a much larger central opening in the core; not only to accommodate the large diameter hoist rope, but also the lateral motion of the rope particularly at the top of the shaft. This need may require the use of non-standard custom-made cores.

In sum, our preliminary findings indicate that an operating frequency in the vicinity of 300 kHz may offer decided performance advantages over that obtainable at substantially higher and lower frequencies. These findings need to be verified and better quantified by conducting a more comprehensive overall systems analysis and optimization, including the effects of electromagnetic noise.